Modification of Anomalous Deposition In Zn-Ni Alloys Using Antimony Additives

By H.-M. Wang and T. J. O'Keefe

Anomalous deposition is commonly encountered with electrogalvanizing alloys such as Zn–Ni, Zn–Co or Zn–Fe. The primary objectives of this study were to develop a better understanding of the fundamental aspects of anomalous behavior in the Zn–Ni system and to investigate means of minimizing such effects during processing. Very low concentrations of either Sb(III) or Sb(V) were found to significantly decrease anomalous behavior in the Zn–Ni alloy deposition. Agitation, current density and temperature were also investigated to determine their effect on the alloy composition and structure. In some instances, with the proper amounts of additives and optimum operating conditions, normal deposition was attainable. A qualitative study using EIS techniques was performed and it was found that the polarization resistance decreased dramatically in the presence of antimony.

Zinc–nickel alloys have been developed to provide an electrogalvanizing coating system with properties superior to those of pure zinc.[1,2] The γ phase alloys with 10 to 15 percent Ni content are known to exhibit excellent corrosion resistance, paintability, formability and weldability.[3–5] The electrochemistry of the deposition process is more complicated, however, because of the anomalous nature of Zn–Ni codeposition, in which the less noble zinc deposits preferentially. Several mechanisms have been proposed to explain this,[6–11] but the hydroxide suppression mechanism appears to be persuasively supported by the experimental evidence.[9–11] According to this mechanism, deposition of Ni is retarded by the zinc hydroxide formed on the cathode as a result of the pH rise in the cathode double layer.

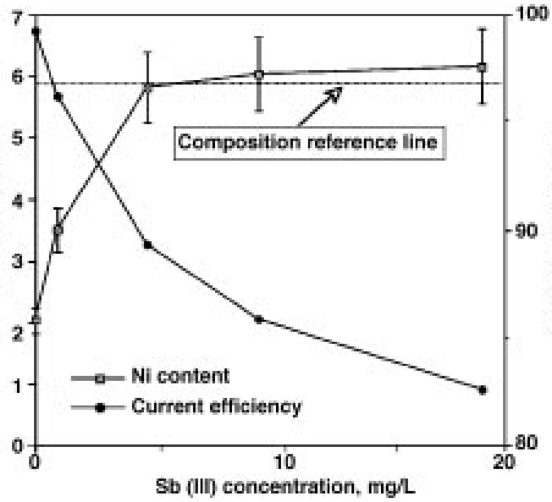

Fig. 1—Effect of Sb(III) on the Ni content and current efficiency of Zn-Ni alloy deposits, using electrolytes containing 80 g/L Zn(II), 5 g/L Ni(II), at pH 1.5, 55 ˚C, 250 mA/cm^2, 60 sec.

Table 1
Comparison of Effect of Sb(III) & Sb(V) On Ni Content and Current Efficiency of Alloy Deposits

Antimony	conc., mg/L	Ni content,%	Current eff., %
Sb(III)	0	2.1	98
	1	3.6	96
	5	5.8	89
	10	6.0	86
	20	6.1	83
Sb(V)	1	2.2	98
	5	2.7	95
	10	3.4	93
	20	4.0	91
	50	4.8	90

Conditions: 80 g/L Zn(II), 5 g/L Ni(II), pH 1.5, 55 ˚C, 250 mA/cm^2, 60 sec, agitation

One of the most pronounced examples of anomalous deposition occurs in acid zinc plating, evidenced by the preferential reduction of the less noble zinc to the more noble hydrogen. It is well accepted that the overpotential for hydrogen gas evolution dominates the nobility predicted by thermodynamics. As a result, one characteristic of the acid zinc plating system is a distinct sensitivity to the catalytic effects of co-deposited species capable of modifying the deposition order. For example, zinc can be plated with relatively high current efficiency from acid sulfate baths only when the electrolyte is relatively free of impurities that lower the hydrogen overpotential.

Antimony is one of the more active species capable of modifying the zinc deposition behavior in acid zinc plating. A depolarization of 20 to 40 mV was observed with 0.1 to 100 mg/L antimony in the electrogalvanizing electrolyte.[12] Additions of antimony also produced progressive nucleation and changed the zinc deposition morphology from highly faceted hexagonal platelets to a rounded, more granular-appearing structure. In the higher acid-level zinc electrowinning electrolytes, antimony at concentrations as low as 10 to 20 ppb can cause dramatic changes in polarization behavior, deposition structure and cause lower current efficiency. It is believed that antimony can either lower the hydrogen overpotential with subsequent gas evolution or form hydrides that serve as the cathodic reaction for localized corrosion and zinc dissolution.[13–16] Accordingly, antimony ions in acid solution are well known promoters of enhanced double layer catalytic activity.

The objective of this study was to develop a better understanding of the fundamental aspects of anomalous behavior and, in particular, the role of low concentrations of antimony (1–50 mg/L) on the Zn–Ni ratio of electrodeposited alloys. Electrogalvanized coatings were made from an electrolyte

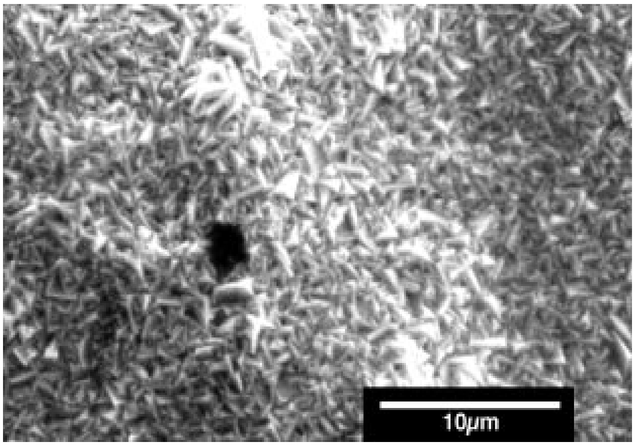

Fig. 2—Morphology of alloy deposit using 80 g/L Zn(II), 5 g/L Ni(II), pH 1.5, 55 °C, 250 mA/cm^2, 60 sec, agitation. Ni content 2.1%.

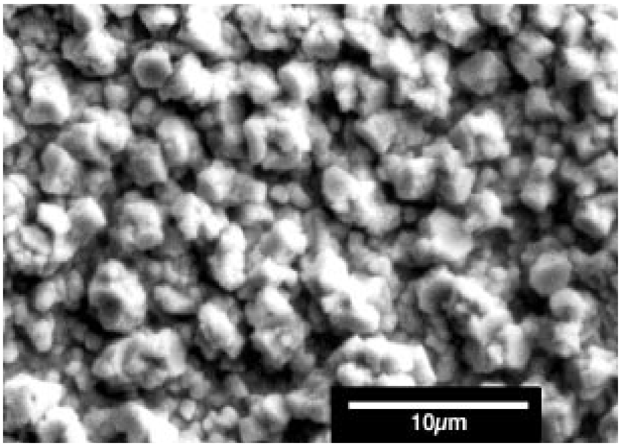

Fig. 3—Morphology of alloy deposit using 80 g/L Zn (II), 5 g/L Ni(II), 5 mg/L Sb(III), pH 1.5, 55 °C, 250 mA/cm^2, 60 sec, agitation. Ni content 5.8%.

containing either Sb(III) or Sb(V) to investigate the effects of the oxidation state on alloy composition, current efficiency and morphology. The results were compared to deposits obtained using an additive-free solution. Polarization resistance was measured by means of the EIS technique to gain some insight into the more qualitative aspects of anomalous behavior and into the catalytic effect of antimony at the cathode. Process parameters such as agitation, pH, plating current density and temperature were also investigated.

Experimental Procedure

Electrolyte Preparation

A zinc sulfate stock electrolyte (pH 5) containing 200 g/L Zn(II) was prepared by dissolving French process zinc oxide with reagent grade sulfuric acid. The solution was then purified, using zinc dust, and filtered. Test solutions were prepared by adding deionized water, sulfuric acid and additives to the stock electrolyte to give the desired composition. Nickel was added as a sulfate solution, while Sb(III) and Sb(V) additions were made as potassium antimony tartrate solution and sodium hexafluoroantimonate solution, respectively.

Electrodeposition

Electrodeposition was conducted in a cell consisting of a 250-mL jacketed beaker fitted with a plexiglass lid. The distance between cathode and anode was 30 mm. Platinum mesh was used as the anode and was installed in a glass tube with a fritted disc to keep the anode products separated from the bulk electrolyte. The reference electrode was a saturated Hg/Hg_2SO_4 electrode (0.656 V vs. SHE) mounted in a Luggin probe filled with 200 g/L H_2SO_4. The cathode substrate was low-carbon steel strip (19 x 63 x 0.76 mm) that was first cleaned ultrasonically in laboratory grade detergent, rinsed with distilled water and dried in a stream of nitrogen. After degreasing with trichloroethylene, it was weighed and masked with electroplater's tape to expose a circular working area of one cm^2. The taped strip was anodically polarized at 100 mA/cm^2 and 60 °C in 15 g/L of an alkaline cleaner for 30 sec, rinsed, dip-pickled in 200 g/L sulfuric acid solution at room temperature for 20 sec and rinsed. The cleaned substrate was then placed in the electrolysis cell to reach the plating temperature.

The cell was connected to a circulating water bath capable of controlling temperatures in the range of 25 to 65 °C. Forced convection was provided by nitrogen sparging. Electroplating was carried out using a potentiostat/galvanostat[a] operated by electrochemical software at current densities from 100 to 500 mA/cm^2. The deposit weight was 50 g/m2 and the deposit thickness was about seven µm. After electrolysis, the cathode was quickly removed from the cell, rinsed with distilled water and dried with nitrogen gas prior to further processing. The surface morphology and composition of the deposit were obtained using a scanning electron microscope with an attached energy dispersive spectrometer.

Electrochemical Impedance Spectroscopy (EIS)

Electrochemical impedance spectroscopy data were obtained with an electrochemical impedance system.[b] Pure zinc was used as the working electrode, with solutions containing 80 g/L Zn(II), pH 4.5 at ambient temperature without additive and with 5 mg/L Sb(III) additions. The working electrode was prepared by wet polishing on 600-grit silicon carbide paper, cleaning in an ultrasonic bath in distilled water and drying in an air stream, then taping to expose a one-cm^2 working area. A lock-in analyzer with a frequency range from 5 Hz to 10^5 Hz and the Fast Fourier Transform technique from 0.5 Hz to 5 Hz were used to generate the impedance plots with 5 mV AC amplitude at 30 mV cathodic potential of the open-circuit potential of the zinc electrode.

Results and Discussion

Effect of Antimony

The effects of Sb(III) additions on Ni content and current efficiency of Zn–Ni alloy deposits are shown in Fig. 1. The composition of the alloys and the metal ratio of the solution are expressed on a weight percentage basis as employed by Brenner.[10] Included in this figure is the alloy "composition-reference line," which represents the condition when the weight percentage of metal in the deposit would be the same as its weight percentage in the electrolyte. Alloys with Ni content lying above the composition reference line indicate that the deposition is the normal type, while alloys with Ni content below this line represent anomalous deposition behavior.

As can be seen in Fig. 1, the Zn–Ni deposition from the additive-free solution was anomalous, because the percentage of the more noble metal Ni in the alloy was much lower

---

[a] Model 273, Princeton Applied Research, Princeton, NJ

[b] Model 378, Princeton Applied Research, Princeton, NJ

than in the solution. It also shows that the current efficiency under such conditions was relatively high, indicating a very small amount of hydrogen evolution.

Table 2
Effect of Agitation & pH on Ni Content of Alloys

Ni Content, wt %

Additives	pH 1.5		pH 4.5	
	No Agitation	Agitation	No Agitation	Agitation
No Sb(III)	2.7	2.1	1.9	1.8
1 mg/L Sb(III)	3.1	3.6	2.8	3.5
5 mg/L Sb(III)	3.7	5.8	3.3	5.7

Conditions: 80 g/L Zn(II), 5 g/L Ni(II), 55 ˚C, 250 mA/cm^2, 60 sec

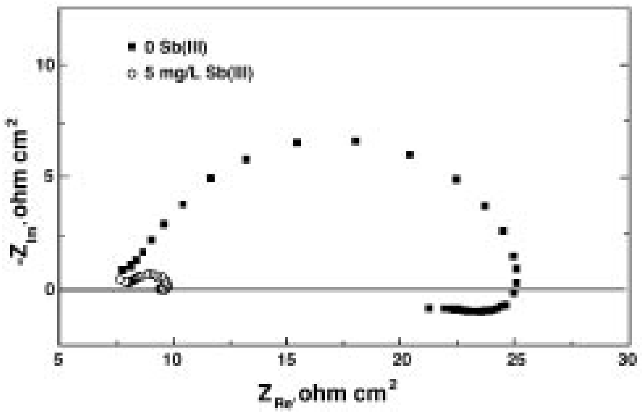

Fig. 4—Comparison of complex plane impedance plots of zinc electrode at -30 mV vs. its open circuit potential, in a solution containing 80 g/L Zn(II), at pH 4.5, with 0 and 5 mg/L Sb(III).

The Ni content increased substantially when Sb(III) was present in the solution. As the Ni content increased with Sb(III) concentration, the current efficiency decreased, indicating that both nickel deposition and hydrogen evolution were enhanced by the presence of the antimony. The exact role of antimony at the cathode is still open to question; however, it may involve reduction from its trivalent state in the form of SbO^+ or $HSbO_2$, followed by the formation of stibine (SbH_3) by the reaction of antimony and hydrogen ions. Stibine may then decompose into antimony and hydrogen, because it is thermodynamically unstable in acid solution when not cathodically polarized.[17,18] Therefore, the continued cyclic formation and decomposition of stibine may allow a relatively low bulk content of antimony to concentrate in the double layer and have a major effect on the overall interfacial reaction.

As discussed previously, the discharge of nickel and hydrogen may be suppressed as a result of the formation and adsorption of zinc hydroxide. When antimony is present in the solution, the uniformity of the hydroxide could be disrupted by the reaction of antimony at the cathode, creating more deposition sites for nickel and hydrogen.

One significant feature seen in Fig. 1 is that normal deposition could be obtained with relatively low Sb(III) concentrations in the range of 5 mg/L. No substantial increase in Ni content was observed when the Sb(III) concentration increased from 5 mg/L to 20 mg/L, indicating that diffusion of Ni ions may also be a factor affecting the alloy composition. On the other hand, current efficiency kept decreasing with increased Sb(III) concentration. Therefore, an optimum Sb(III) concentration appears to exist and is a function of the electrolyte composition and operating parameters, such as electrolyte transport or agitation, pH and chemical composition.

The Sb(III) had a notable effect on the alloy morphology as well. The deposit obtained from the additive-free electrolyte contained about 2.1 percent Ni, was relatively smooth, with a silver gray appearance, and consisted of sharply angular facets growing at random angles to the substrate (Fig. 2). The deposit obtained from an electrolyte containing 1 mg/L Sb(III) had a 3.6 percent Ni content, was darker gray in color and was dense and continuous, but had some randomly located, isolated crystals growing on the surface. With 5 mg/L Sb(III) in the electrolyte, the Ni content was 5.8 percent; the deposit was visually darker as a result of the rougher growth and more nodular appearance, as seen in Fig. 3. Increased Sb(III) concentration, up to 20 mg/L, resulted in a deposit containing about 6 percent Ni, and the deposition morphology was more powdery than that of the deposit obtained at a lower concentration.

Electrochemical Impedance Spectroscopy (EIS)

As mentioned previously, the anomalous deposition behavior observed in the Zn–Ni alloy system is influenced primarily by the kinetic factors related to the presence of inhibiting cathode surface films. The double layer phenomenon involves two main interfacial processes: (1) double layer charging and (2) faradaic processes caused by the electrochemical reactions occurring. AC impedance spectroscopy techniques have been used effectively to investigate surface reactions of the type occurring during electrogalvanizing.[19,20] Because the antimony additions had such a dominant effect on increasing the Ni content in the deposit, some qualitative tests were made, using EIS, to determine if changes could be detected when antimony was present in the electrolyte. No attempts were made to define any specific mechanisms or to model the system, using equivalent electrical circuits. More extensive studies would be required to adequately characterize the Zn–Ni system and will be conducted at a later date. Therefore, only the major features of the observed impedance plots and some possible causes for the responses will be given.

AC impedance spectroscopy of a pure zinc electrode at the potential 30 mV cathodic to its open circuit in zinc sulfate solutions containing 80 g/L Zn(II) at pH 4.5 with 0 and 5 mg/L Sb(III) is shown in Fig. 4. The impedance plot obtained in the addition-free solution gave a polarization resistance of about 25 ohms. At low frequencies, an inductive loop appears, probably corresponding to the formation and adsorption of intermediate insoluble products, such as oxides or hydroxides.[20,21] Similar diagrams were obtained by other investigators from both sulfate and chloride electrolytes.[20–22] The polarization resistance decreased dramatically with an addition of 5 mg/L of Sb(III), as seen in Fig. 4. Although not specifically definitive in terms of identifying the changes occurring in surface chemistry, the data obtained are consistent with the previous results and could indicate that disruption of the polarizing films is occurring as a result of the presence of antimony. The amount of hydrogen observed visually at the electrode surface also increased when Sb(III) was present in the solution, another indication that the anomalous behavior was decreasing.

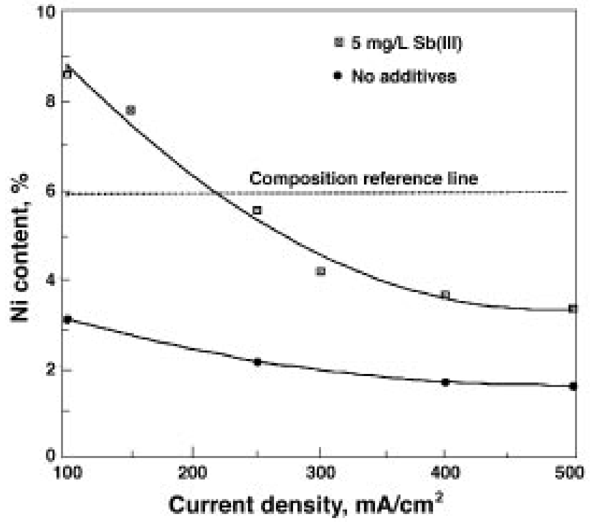

Fig. 5—Effect of current density on the content of Zn-Ni alloy deposited from a solution containing 80 g/L Zn(II), 5 g/L Ni(II), 5 mg/L Sb (III), at 55 ˚C, agitation.

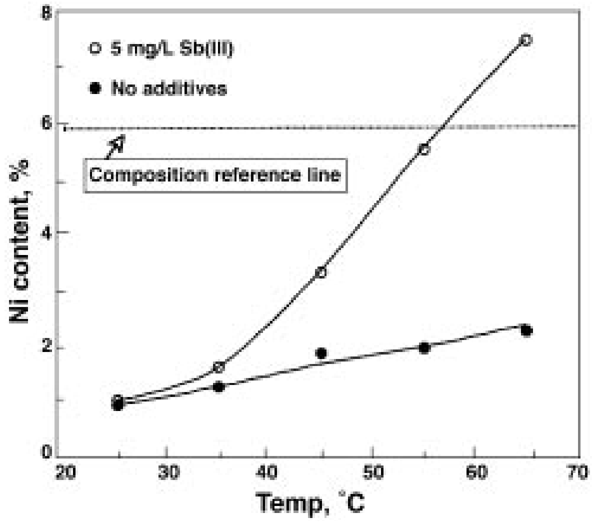

Fig. 6—Effect of temperature on the Ni content of deposits, using 80 g/L Zn (II), 5 g/L Ni (II), 5 mg/L Sb(III), 250 mA/cm², 60 sec, agitation.

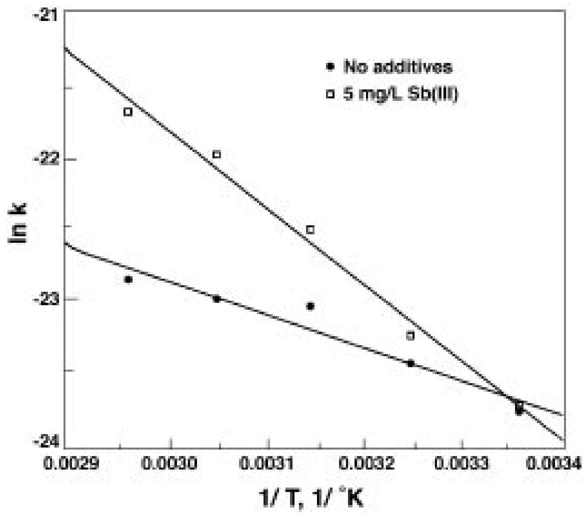

Fig. 7—Arrhenius plot for rates of nickel deposition, using 80 g/L Zn(II), 5 g/L Ni(II), with (l) no additives, and (q) 5 mg/L Sb(III).

Effect of Antimony Oxidation State

In zinc electrowinning, it has been reported that the antimony oxidation state influences the activation overpotential, zinc deposit morphology and plating current efficiency.[16] Both Sb(III) and Sb(V) cause depolarization, but Sb(III) appears to be the more potent of the two depolarizers. The effects of Sb(III) and Sb(V) on the alloy composition and plating current efficiency for Zn–Ni films were studied and the morphologies of the deposits obtained with Sb(V) additions were investigated. Comparison of the effects of Sb(III) and Sb(V) on the Ni content is shown in Table 1. The results show that Ni deposition was enhanced by both Sb(III) and Sb(V) additions, and that the Ni content increased with increasing antimony concentration in the solution. When each was present at the same concentration, however, the Ni content of the alloys was higher with Sb(III) than with Sb(V).

Effect of Plating Parameters

The effects of various operating parameters on the composition and structure of the deposits with Sb(III) (5 mg/L) were investigated. No attempt was made to provide a detailed characterization of the effect of plating parameters on alloy deposition. Changing the pH of the electrolyte from 1.5 to 4.5 had no significant effect on the results.

Agitation: The effect of solution agitation on Ni content is shown in Table 2. Without antimony, the Ni content of the deposits decreased with increased agitation. When Sb(III) was added, however, the Ni content increased with increasing agitation. At such low concentrations, the Sb(III) ions are assumed to be under diffusion control. Agitation reduces the diffusion layer thickness, allowing the limiting current density of antimony ion to increase. Agitation also seemed to reduce the degree of nodulation and gave more uniform deposits.

Current density: The Ni content decreased with increasing current density in both additive-free and 5 mg/L Sb(III)-containing electrolytes, as shown in Fig. 5. The Ni content of the deposits was higher, however, for electrolytes containing Sb(III) than for the additive-free electrolytes. These data indicate that the catalytic effect of antimony is governed by diffusion. For constant agitation, the reaction rate of Sb(III) and nickel deposition is nearly constant, while the zinc deposition rate increased with increasing current density and is probably under activation control.

Temperature: Temperature may have two effects on electrogalvanizing Zn–Ni alloys.[6] Increasing temperature (1) increases the rate of diffusion of antimony ions and, if under diffusion control, increases the limiting current density of Sb(III), and (2) depolarizes the metal deposition and hydrogen evolution reactions. Usually, the degree of depolarization is larger for the more noble metal. Both effects favor the deposition of nickel and, as shown in Fig. 6, the Ni content of the alloys increased with temperature. The rate of change of the nickel content with temperature is also much greater when the additive is present. Arrhenius plots for the rates of nickel deposition are shown in Fig. 7. Without additives, the activation energy of nickel deposition calculated from the slope is 4.7 kcal/mol, indicating that the reaction is under diffusion control. The step in question may be for movement of nickel ions though the zinc hydroxide film. With antimony additions, the activation energy of nickel deposition is 10.8 kcal/mol, which implies that the reaction is more likely under activation control. In this case, the hydroxide film may be disrupted sufficiently that charge transfer becomes the rate-controlling factor for nickel deposition. Further study is required to determine the reaction rates and mechanisms for each species present in the electrolyte and the general trends to show that the Sb(III) does modify or alter the reaction mechanism.

Conclusions

Because the electrodeposition of Zn-Ni alloys from the sulfate solution is anomalous, reduction of both nickel and hydrogen ions is inhibited, resulting in a low Ni percentage in the deposit. The Ni content of the alloys increased significantly with Sb(III) additions up to 5 mg/L, where the deposition mechanism became nearly normal. Further additions of antimony increased the Ni content slightly; however, the current efficiency continued to decrease as a result of increasing hydrogen evolution. An optimum Sb(III) concentration appears to exist, and which is a function of electrolyte composition and operating parameters. The morphology of the alloys produced in the presence of Sb(III) was less uniform in size and shape, with a more clustered appearance as the Sb(III) concentration increased. The addition of Sb(V) also increased the Ni content and decreased the current efficiency, but to a lesser extent than Sb(III).

Qualitative tests using the EIS technique revealed the possible formation and adsorption of an insoluble hydroxide at the interface between the zinc electrode and the electrolyte. The polarization resistance decreases dramatically even with low Sb(III) additions, suggesting that the adsorbed layer may be disrupted. The calculated activation energies also indicated that Sb(III) changed the deposition mechanism.

Agitation of the electrolyte with Sb(III) additions increased the Ni content of the alloys and produced more uniform deposits compared to the ones without agitation. Increasing temperature and decreasing current density gave higher Ni content, but less dense deposits.

The data obtained in this study indicate that low levels of antimony additions can be used to substantially modify the anomalous behavior of Zn–Ni alloy deposition and to vary the structure of the deposit. The process parameters can also be used to control the alloy composition and structure. Even though normal deposition can be obtained, however, the alloy structure and current efficiency are not necessarily improved. Fundamental studies are needed to advance further the electrocrystallization aspects of the process. Optimization experiments on the antimony level, with plating conditions needed to produce high quality alloys, would be necessary. Further studies on the influence of the oxidation state and chemical form of antimony would also be desirable. Overall, the use of such additives offers some potentially interesting and unique ways to modify the quality and structure of zinc alloys, as well as providing a better understanding of the basic mechanisms operative during anomalous deposition.

Editor's note: *Manuscript received, August 1993.*

Acknowledgments

Financial support from Inland Steel, E. Chicago, IN and extensive technical assistance and guidance from Dr. H. Lee, W. Carter and Dr. M. Blaser and others at the Inland Research Laboratories, and the matchimg grant from the Manufacturing Research and Training Center, UMR, Rolla, MO are gratefully acknowledged.

References

1. *Trans. Iron Steel Inst. Japan*, Special Issue on Automotive Precoated Sheet Steels, 23 (Nov. 1983).
2. AESF Fourth Continuous Strip Plating Symp., Chicago, IL (1984).
3. A. Shibuya, T. Kurimoto, Y. Hoboh and N. Usuki, *Trans. ISIJ*, **23**, 923 (1983).
4. N. Miura, T. Saito, T. Kanamaru, Y. Shindo and Y. Kitazawa, *ibid*., 913 (1983).
5. S. Wakano, N. Suzuki, Y. Hoboh and R. Nomi, *Proc. Int'l. Conf. on Zinc and Zinc Alloy-Coated Steel Sheet (Galvatech)*, The Iron and Steel Institute of Japan, 289 (1989).
6. A. Brenner, *Electrodeposition of Alloys: Principles and Practice*, Vols. I and II, Academic Press, New York, NY, 1963.
7. D.E. Hall, *Plat. and Surf. Fin*., **70**, 59 (Nov. 1983).
8. L. Felloni, R. Fratesi, E. Quarini and G. Roventi, *J. Applied Electrochem.*, **17**, 574 (1987).
9. K. Higashi, H. Fukushima, T. Urakawa, T. Adaniya and K. Matsuko, *J. Electrochem. Soc.*, **128**, 2081 (1981).
10. H. Fukushima, T. Adaniya, K. Higashi, R. Kammel and M. Karimkhani, *Metall*, **42**, 242 (1988).
11. H. Fukushima, *Galvatech, ISIJ*, Tokyo, 19 (1989).
12. V. Srinivasan, PhD Thesis, Univ. of Missouri-Rolla (1987).
13. D.J. Robinson and T.J. O'Keefe, *J. Appl. Electrochem*., **6**, 1 (1976).
14. B.A. Lamping and T.J. O'Keefe, *Metall Trans.*, **7B**, 551 (1976).
15. M. Maja, N. Penazzi, E. Fratesi and G. Roventi, *J. Electrochem. Soc.*, **129**, 2695 (1982).
16. R.K. Singh, PhD Thesis, Univ. of Missouri-Rolla (1985).
17. A.L. Pitman, M. Pourbaix and N. de Zoubov, *J. Electrochem. Soc.*, **104**, 594 (1957).
18. V. Past, Encyclopedia of Electrochemistry of the Elements, A.J. Bard, Ed., Marcel Dekker, New York and Basel, 1975; Ch. IV–1.
19. Y. Imai and M. Kurachi, *Denki Kagaku*, **47**(2), 89 (1979).
20. A. Jardy, R. Rosset and R. Wiart, *J. Appl. Electrochem.*, **14**, 537 (1984).
21. L. M. Baugh, *Electrochimica Acta*, **24**, 657 (1979).
22. C. Cachet and R. Wiart, *J. Electroanal. Chem.*, **111**, 235 (1980).

About the Authors

Dr. Hung-Ming Wang is currently a senior plating engineer for AMP-Taiwan, No. 6, Industrial East V Road, Science-Based Industrial Park, Hsin-Chu, Taiwan. He is involved in electrodeposition of nickel, palladium-nickel, gold, tin-lead and the development of continuous plating processes for electronic connector manufacture. He holds a PhD in metallurgical engineering from the University of Missouri-Rolla.

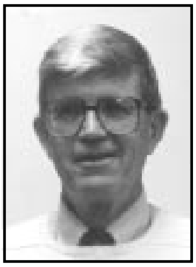

Dr. Thomas J. O'Keefe is Curators' Professor of Metallurgical Engineering and Senior Investigator, Materials Research Center, University of Missouri-Rolla (UMR). He holds a PhD in metallurgical engineering from UMR and has held various industrial positions. His research interests are in deposition processes, corrosion and chemical metallurgy.